Journal of Solid State Chemistry 185 (2012) 264–270

Contents lists available at SciVerse ScienceDirect

Journal of Solid State Chemistry

journal homepage: www.elsevier.com/locate/jssc

Rapid Communication

Ab initio study of the linear and nonlinear optical properties of chalcopyrite $CdGeAs_2$

You Yu [a], Beijun Zhao [a,*], Shifu Zhu [a], Tao Gao [b], Haijun Hou [a], Zhiyu He [a]

[a] College of Materials Science and Engineering, Sichuan University, Chengdu 610064, China
[b] Institute of Atomic and Molecular Physics, Sichuan University, Chengdu 610065, China

ARTICLE INFO

Article history:
Received 19 July 2011
Received in revised form
4 October 2011
Accepted 9 October 2011
Available online 15 October 2011

Keywords:
$CdGeAs_2$
GW
Linear optical
Nonlinear optical

ABSTRACT

We present an *ab initio* theoretical study of the electronic, linear and nonlinear optical properties of $CdGeAs_2$ using a pseudopotential plane-wave method. Specifically, we evaluate the band structure, density of states, charge density, the dielectric function $\varepsilon(\omega)$ and the second harmonic generation response susceptibility $\chi^{(2)}_{312}(-2\omega;\omega,\omega)$ over a large frequency range. As LDA underestimates the band gap, we have applied the GW approximation method to calculate the quasiparticle band structure and obtain an energy band gap in agreement with experiment. In this case the opening of the gap due to the GW correction can be used as scissor shift to calculate the linear and nonlinear optical properties. The intra- and inter-band contributions to the imaginary part of $\chi^{(2)}_{312}(-2\omega;\omega,\omega)$ are presented over a broad energy range. It is found that the small energy gap semiconductor $CdGeAs_2$ has larger values of $\varepsilon_1(0)$ and $\chi^{(2)}_{312}(0)$ than other chalcopyrite structures.

1. Introduction

Cadmium germanium arsenide ($CdGeAs_2$) is an important ternary chalcopyrite structure semiconductor, standing out because of its extremely high second-order nonlinear optical coefficient (d_{36}=236 pm/V) combined with adequate birefringence for phase matching and wide infrared transparency range (2.4–18 μm) [1]. These properties make this material very promising for the generation of mid-infrared frequencies using second harmonic generation (SHG) and a CO_2 laser. $CdGeAs_2$ is a narrow direct-gap semiconductor, and the band gap of this material is about 0.57 eV [2] at room temperature and about 0.67 eV [3] at liquid helium temperature. Laser devices have been reported [4–7] using large, crack-free, single crystals grown by the horizontal gradient freeze (HGF) technique [8–11]. Although laser devices have been reported using $CdGeAs_2$ crystals, absorption losses due to defects are still a major limitation for the efficiency of the devices [5–7].

There have been several experimental studies of the structural [12–18] and electronic [2,3,19–22] properties of this material, as well as a number of investigations of the linear [1,23–35] and nonlinear [1,36,37] optical response. However, theoretical efforts have been primarily concerned with ground state properties [22,38–46]. While there has been some work on linear optical response [1,45], the only full band structure calculation of nonlinear response has been restricted to zero frequency [1]. In this context, it would be useful to have a comprehensive analysis of the linear and nonlinear optical properties of $CdGeAs_2$, as determined from first principles, over a broad energy range.

So far, first principle calculations have been successfully used to obtain different properties of chalcopyrite structure semiconductors, such as structural, electronic, linear and nonlinear optical properties [37,45,47–52]. It is well known that the band gap calculated by generalized gradient approximation (GGA) and local density approximation (LDA) is generally smaller than the experimental data. The error is due to the discontinuity of exchange-correlation energy. In order to get the optical spectrum and make a realistic comparison with experiments one needs to correct for this. This can be achieved in two ways. The scissors shift is normally chosen to be the difference between the experimental and theoretical band gap and is used to shift the conduction bands only. Another way in which you do not have to rely on experimental data is to determine the self-energy using GW approximation [53] (GWA, G is the Green's function, W is the screened coulomb interaction). In this case the opening of the gap due to the GW correction can be used as scissor shift. Many researchers have adopted the first method. It is worth mentioning that Rashkeev et al. [37] investigated the birefringence and the frequency-dependent SHG coefficients of $CdGeAs_2$ using the linear muffin-tin orbitals (LMTO) method within the atomic sphere approximation, and the scissors shift has to rely on experimental gap in their work. In our work, we calculate the quasiparticle band structure of $CdGeAs_2$ by using GW method and obtain an energy gap

* Corresponding author. Fax: +86 28 85412745.
E-mail address: bjzhao@scu.edu.cn (B. Zhao).

0022-4596/$ - see front matter © 2011 Elsevier Inc. All rights reserved.
doi:10.1016/j.jssc.2011.10.014

in agreement with experiment. Then the corrected gap is used to calculate the linear and nonlinear optical properties.

In this paper we present a first-principles calculation of the electronic structure, linear and nonlinear optical properties for $CdGeAs_2$ using the plane-wave pseudopotential method. Specifically, we evaluate the dielectric function $\varepsilon(\omega)$ and the SHG response coefficient $\chi^{(2)}(-2\omega;\ \omega,\ \omega)$ over a large frequency range. The paper is organized in the following way. In Section 2, we give details of our calculations. The electronic ground state properties, quasiparticle band structure, linear and nonlinear optical susceptibilities are presented and discussed in Section 3. In Section 4, we summarize our conclusions.

2. Computational details

In this work, all the structural optimizations and property calculations are performed using a plane-wave pseudopotential implementation of density functional theory (DFT) within the LDA implemented in the code ABINIT [54]. It relies on an efficient fast Fourier transform algorithm [55] for the conversion of wave functions between real and reciprocal spaces, on an adaptation to a fixed potential of the band-by-band conjugate-gradient algorithm [56], and on a potential-based conjugate-gradient method [57] for the determination of the self-consistent potential. The interaction between the valence electrons and the nuclei and core electrons is described by Troullier–Martins type norm-conserving pseudopotentials which have been generated thanks to the FHI98PP code [58]. The exchange-correlation energy is evaluated in local density approximation (LDA), using Perdew–Wang parametrization [59] of Ceperley–Alder electron-gas data [60]. Both Ge and As pseudopotentials include the 4*s* and 4*p* in valence, for Cd pseudopotential, 4*d* and 5*s* are taken as the valence states.

All the calculations involve an eight-atom tetragonal primitive cell. The original lattice constants and internal coordinate used in our calculations are taken from the experimental values. For the optimizations, *k*-point sampling of $4\times4\times4$ Monkhorst–Pack grids are used and the plane-wave cutoff of 22 hartree are chosen. Convergence tests show that the Brillouin zone (BZ) sampling and the kinetic energy cutoff are sufficient to guarantee an excellent convergence. The structural parameters are obtained by optimizing lattice constants and atomic coordinates until all force components are below 5×10^{-5} Ha/Bohr. After geometry optimizations, the relaxed structures are used in the electronic structure and optical response-function (RF) calculations to obtain the band structure, density of states (DOS), charge density, and dielectric function and second-order non-linear optical susceptibilities.

We first obtain the electronic ground state properties using DFT within the LDA. The results tell us that $CdGeAs_2$ is a direct band gap semiconductor material. In the band structure, the Gamma (Γ) point is corresponding to the conduction band minimum (CBM) and valence band maximum (VBM). As is known, the Kohn–Sham eigenvalues in the LDA approximation do not give the quasiparticle energies correctly. When the optical response calculation is made, thus the self-energy effects must be included. Otherwise the unoccupied conduction bands have no physical significance and a band gap problem appears: the absorption starts at too low an energy. In order to take into account the self-energy effects, a scissors approximation [61,62] is usually used to shift upward all the conduction bands in order to agree with measured values of the band gap. We have corrected the band gap at the Γ point using GW approximation.

The detailed formalism for the determination of the linear dielectric tensor and the susceptibility for the SHG have been presented in Sipe and Shkrebtii [63]. All the calculations are converged in terms of basis functions as well as in the size of the *k*-point mesh representing the Brillouin Zone (BZ). In the linear optical properties as well as second-order susceptibility calculations, the irreducible BZ has been sampled with a $8\times8\times8$ Monkhorst–Pack grid.

3. Results and discussion

3.1. Structural optimization

As is well known, the crystal structure of $CdGeAs_2$ is described by space group $I\bar{4}2d$ and point group $\bar{4}2m$. Generally, the II–IV–V_2 chalcopyrites are analogous to the widely studied III–V materials GaP and GaAs, except that the chalcopyrite structure is tetragonally distorted from the simpler zinc-blende structure of the III–V compounds. We have recently presented results on the structural properties of $CdGeAs_2$ [46]. The calculated equilibrium values of the structural parameters, namely *a*, *c*/*a* and *u*, for $CdGeAs_2$ are 5.912 (in Å), 1.887, and 0.2781 in the LDA approximation. Our calculations underestimate the equilibrium lattice parameter *a*(*c*) with the maximal error of 0.51–0.58% (0.50–0.60%) with respect to experimental values, a normal agreement by LDA standards. This is largely sufficient to allow the further study of electronic, linear and nonlinear optical properties for $CdGeAs_2$.

3.2. Electronic ground state

3.2.1. Band structure

The band structure of $CdGeAs_2$ along the lines of high symmetry points in the BZ are shown in Fig. 1 and the Fermi level (E_f) is set to zero. These special points in *X* axle represent the high symmetry points in the BZ, and for $CdGeAs_2$ with the tetragonal structure, $Z=(0.5,\ 0.5,\ -0.5)$, $\Gamma=(0,\ 0,\ 0)$, $X=(0,\ 0,\ 0.5)$, $P=(0.25,\ 0.25,\ 0.25)$, $N=(0,\ 0.5,\ 0)$. Both the VBM and CBM are at Γ point, so $CdGeAs_2$ has a direct band gap with the calculated value to be 0.16 eV. This result is the same as that obtained in Ref. [45], but it is severe underestimation compared with the experiment value [2]. When the spin–orbit interaction is not included in the calculation, the lower three CB states counting from the CBM are Γ_1, Γ_3, and Γ_2. The energy splitting between Γ_2 and Γ_3 is 0.43 eV, larger than 0.20 eV predicted by Madelon et al. [22] and closer to 0.46 eV calculated by Limpijumnong and Lambrecht [43]. The top of the valence band consists of two levels with symmetry Γ_4 and Γ_5, and the latter is doubly degenerated. The two levels originate from the same triply degenerate Γ_{15} level of the zinc-blende

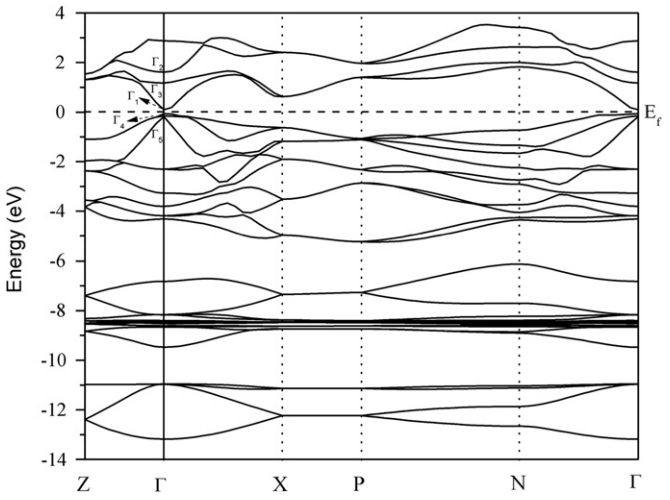

Fig. 1. Band structure of $CdGeAs_2$.

structure. With the use of the sign convention of Ref. [64], the crystal-field (CF) splitting between them is given by $\Delta_{CF}=\varepsilon(\Gamma_5)-\varepsilon(\Gamma_4)$. It represents the effects of the (i) existence of two distinct cations Cd and Ge, (ii) tetragonal distortion $c/2a\neq 1$, and (iii) anion As displacement $u\neq 1/4$. In the zinc-blende structure ($c/2a=1$, $u=1/4$) one has $\Delta_{CF}=0$, and the $\Gamma_5+\Gamma_4$ pair forms the triply degenerate state at VBM. Any of the three factors (i)–(iii) can lead to $\Delta_{CF}\neq 0$. Our calculated value Δ_{CF} for the compound is 0.12 eV and the corresponding experimental value is reported to be 0.21 eV [64].

3.2.2. Total and partial density of states

In order to analyze the electron distribution of each atomic orbital, we calculate the total DOS and partial density of states (PDOS). Fig. 2 shows that the valence band of $CdGeAs_2$ can be divided into three zones: a deep valence band at around -13 to -11 eV is mainly formed by As 4*s* bonding states which appears to be hybridized with the Cd and Ge orbitals, a middle zone from -9 to -6 eV is mostly composed of the Cd 4*d* states and the upper valence band at higher energy is mostly derived from the anion As 4*p* states hybridized with the cations Cd 5*s*, Cd 5*p* and Ge 4*p* states. We find that the top of valence band and the bottom of conduction band consist mainly of the As atoms. Since As evaporates easily in the experiment, the band gap could be changed for the single crystal, which can be grown from $CdGeAs_2$ polycrystal that is synthesized according to the stoichiometric ratio, and further affects optical transmittance. Therefore, the amount of As could be increased during the synthesis, deviating from the stoichiometric ratio.

3.2.3. Charge density

To visualize the nature of the bond character, we calculate the total electronic charge density on the (110) plane of $CdGeAs_2$ depicted in Fig. 3. In previous papers, we find that the charge density around the cation is spherical [47,48,65]. The same situation is met by the crystal $CdGeAs_2$. Obviously, the charge density around Cd is also spherical. From Fig. 2, we can see that the middle zone (from -9 to -6 eV) is mostly composed of the Cd 4*d* states, so the valence charge density is considerably high and strongly localized around Cd. As we all know, an electron density plot is useful because it represents the electron distribution in an orbital and reflect the

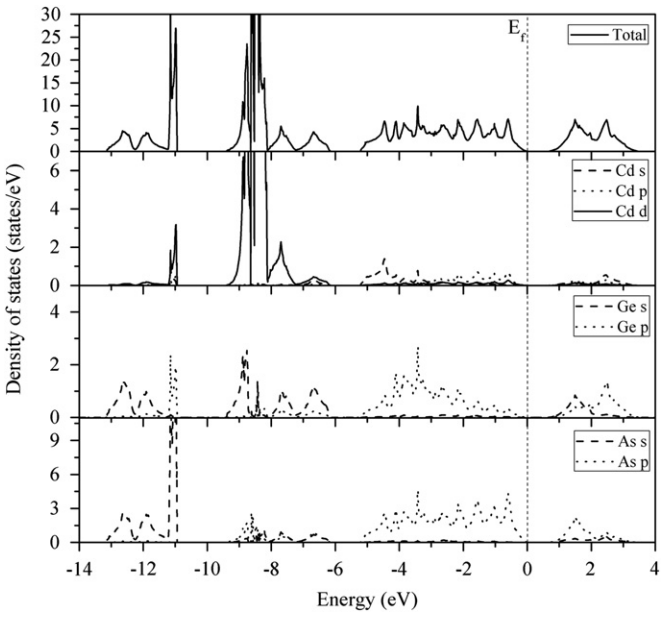

Fig. 2. Total and partial density of states (DOS and PDOS) for $CdGeAs_2$.

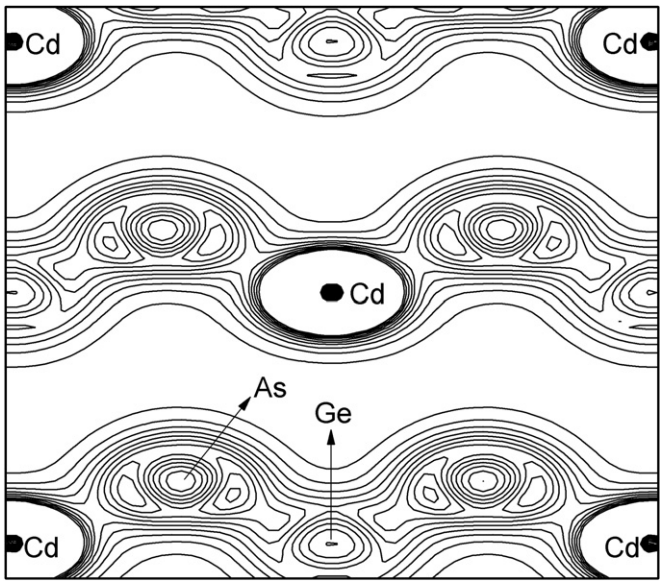

Fig. 3. Calculated electronic charge density on the (110) plane of $CdGeAs_2$.

interactions between bonding atoms. Fig. 3 shows that there are apparent electron density overlaps between Cd and As atoms as well as Ge and As atoms which suggests that the Cd–As bond and Ge–As bond in $CdGeAs_2$ have covalent character. This result is consistent with the PDOS study. In the inner density contour, the Cd atom is connected with the As atom, but the Ge atom and As atom are not connected. This fact indicates that the bonds of Cd–As have more covalent character than those of Ge–As.

3.3. Quasiparticle excitations

The DFT-LDA approximation is very useful to describe the electronic ground state of materials. However, the DFT band structure fails to give reliable quantitative values for the band gaps of insulators and semiconductors, which are often underestimated by as much as 1.0 eV or more. In the present work, we adopt the GW approximation to correct DFT gaps. In order to study the quasiparticle excitation energies, we need to go beyond the LDA approximation. We have a rigorous formulation of the quasiparticle properties in the context of the one-particle Green's function approach. The eigenvalue and wave function of a quasiparticle in a crystal are obtained in this framework by solving the Dyson equation [66]:

$$[E_k(\omega)-H_0(r;\omega)]\varphi_k(r,\omega)-\int dr'\Sigma(r,r';\omega)\varphi_k(r';\omega)=0, \quad (1)$$

where the H_0 includes the kinetic-energy operator, potential due to the ions and the Hartree potential of the electrons. In the GWA, the self-energy Σ becomes

$$\Sigma(r,r';\omega)=i\int\frac{d\omega'}{2\pi}G(r,r';\omega+\omega')W(r,r';\omega')e^{i\delta\omega'} \quad (2)$$

where $G(r,r';\omega+\omega')$ is the full Green's function and $\delta=0^+$ $W(r,r';\omega')$ is the dynamically screened Coulomb interaction given by

$$W(r,r';\omega)=\int d^3r''\varepsilon^{-1}(r,r'';\omega)V(|r''-r'|), \quad (3)$$

where $\varepsilon^{-1}(r,r'';\omega)$ is an inverse dielectric matrix and $V(|r''-r'|)$ is a bare Coulomb potential.

The one-particle Green's function G is constructed using the LDA eigenfuctions and eigenvalues as a starting point and then iteratively updated using the real parts of the quasiparticle

energies from Eq. (1). In this approach, the quasiparticles for semiconductors are on the assumption that the lifetime is infinite. To screen Coulomb interaction, we use a generalized form of the Levine–Louie model dielectric matrix extended to finite frequencies using a generalized plasmon-pole model. This model dielectric function is known to give reliable results for various semiconductors and requires only the dielectric constant ε_∞ as an input. Of course, this can be evaluated from *ab initio* calculations. Once the self-energy operator Σ is constructed, the quasiparticle energies are calculated as

$$E^{qp}_{n,k} = \varepsilon_{n,k} + \langle n,k|\Sigma - V_{XC}|n,k\rangle, \quad (4)$$

where V_{XC} is the LDA exchange-correlation potential. Here, we make use of the fact that the quasiparticle wave functions are extremely well approximated by the LDA wave functions.

For GWA, a converged ground-state calculation on an optimized structure was first performed. In essence, these calculations were carried out to first obtain a self-consistent density and potential Kohn–Sham eigenvalues and eigenfunctions at the ground electronic state. Calculations were performed on grids of reciprocal space points (k points) that included band points at extrema. This was followed by computation of the independent-particle susceptibility matrix at two frequencies and a calculation of the susceptibility matrix, the dielectric matrix, and its inverse. The self-energy matrix elements were then evaluated at selected k points, which then used to derive the GWA eigenvalues for the selected states around the highest occupied states. Because $CdGeAs_2$ is a direct-gap semiconductor, we correct the band gap for the Γ point only. Specifically, 30 electronic bands were used to generate the Kohn–Sham band structure and 90 bands were used in the screening calculation. An energy cutoff of 8 hartree was used in the calculation of the screening matrix. For the calculations of the self-energy matrix elements, 100 bands with an energy cutoff of 6 hartree were adopted to represent the wave functions. Though the screening calculation is very time-consuming, it is still feasible. So, we did not weaken the parameters found in the previous convergence studies. As it is expected, GW corrections widened the energy gaps. The calculated energy gap is 0.35 eV at Γ point. This is substantially larger than the LDA value of 0.16 eV and closer to the experimental value of 0.57 eV [2]. The gap due to the GW correction can be used as a scissor shift to calculate the linear and nonlinear optical properties.

3.4. Linear optical response

The most important measurable quantity we address in this section is the dielectric function $\varepsilon(\omega)$ of the compound, which is a complex quantity. The optical properties of the material are determined by the dielectric function $\varepsilon(\omega)$ given by $\varepsilon(\omega)=\varepsilon_1(\omega)+i\varepsilon_2(\omega)$. The imaginary part of the dielectric function, $\varepsilon_2(\omega)$ depends on the joint density of states and the momentum matrix elements. Due to the tetragonal symmetry, the dielectric functions are resolved into two components $\varepsilon_{2xy}(\omega)$, which is the average of the spectra for polarizations along the x and y directions (electric field perpendicular to the c-axis) and corresponding to the z direction (electric field parallel to the c-axis).

We present the average dielectric function for simplicity ($\varepsilon_1(\omega)=(\varepsilon_{1x}(\omega)+\varepsilon_{1y}(\omega)+\varepsilon_{1z}(\omega))/3$, $\varepsilon_2(\omega)=(\varepsilon_{2x}(\omega)+\varepsilon_{2y}(\omega)+\varepsilon_{2z}(\omega))/3$). The optical properties of solids can be described by means of the transverse dielectric function $\varepsilon(\omega)$. There are two contributions to $\varepsilon(\omega)$, namely intraband and interband transitions. The contribution from intraband transitions is important only for metals. The interband transitions of the frequency dependent dielectric functions can be split into direct and indirect transitions. In this paper, we neglect the indirect interband transitions involving scattering of phonons assuming that they give a small contribution to the frequency dependent dielectric functions. To calculate the contributions of the direct interband to the imaginary parts of the dielectric functions, it is necessary to sum up all possible transitions from the occupied to the unoccupied states taking the appropriate transition dipole matrix elements into account.

A dense mesh of uniformly distributed k-points is necessary in our calculations of the optical properties. Our optical properties are scissors corrected by 0.19 eV. This value is the difference between the calculated energy gap (0.16 eV) by LDA and the corrected energy gap (0.35 eV) by GWA. Since the optical spectra have been analyzed for an energy range 0–20 eV, the spectra contain many peaks which correspond to electronic transitions from the valence band to the conduction band. The values of peaks of the imaginary part of the frequency dependent dielectric function which are labeled with letters in Fig. 4(b) are summarized in Table 1. Through the calculated electronic band structures and density of states, we can explain the different peak structures seen in Fig. 4. The spectra can be divided into two major groups of the peaks, the first from 2 to 5 eV and the second after 5 eV. The first group is dominated by Cd-*sp* and Ge-*sp* transitions, where the first direct interband transition arises between the VBM and CBM, and the first peak (at 2.69 eV) is clearly due to the Γ direction of the BZ. The second group of the peaks is deduced from the Ge-*sp* transitions, where the main peak is located at 5.62 eV, and mainly arises from the N direction of the BZ.

The real part of the dielectric function $\varepsilon_1(\omega)$ is calculated by using the Kramers–Kronig relations [67]. The results of our calculated $\varepsilon_1(\omega)$ spectra are shown in Fig. 4(a). The most important quantity is the zero frequency limit $\varepsilon_1(0)$, which is the electronic part of the static dielectric constant that depends strongly on the band gap. The calculated $\varepsilon_1(0)$ is compared with both experimental and theoretical data in Table 2. We note that a smaller energy gap E_g yields a larger $\varepsilon_1(0)$ value [48–50,70–72].

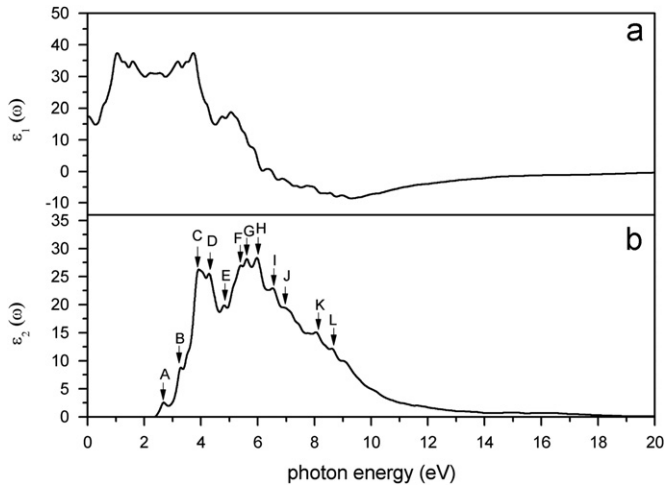

Fig. 4. Calculated (a) real and (b) imaginary part of the dielectric function $\varepsilon(\omega)$ of $CdGeAs_2$.

Table 1
Main peak positions (in eV) of the imaginary part $\varepsilon_2(\omega)$.

Imaginary part	Peaks (eV)											
	A	B	C	D	E	F	G	H	I	J	K	L
ε_2	2.69	3.30	3.93	4.29	4.82	5.40	5.62	5.97	6.53	6.88	8.05	8.61

Table 2
Calculated static dielectric constants of $CdGeAs_2$ compared with both experimental and theoretical data.

Static dielectric constant	This work	Theor.	Expt.		
$\varepsilon_1(0)$	17.28	14.98[a]	18.7 ± 0.5[b]	15.0[a]	16.2[c]

[a] Ref. [68].
[b] Ref. [24].
[c] Ref. [69].

This can be explained on the basis of the Penn model [73]. The Penn model is based on the expression $\varepsilon(0)\approx 1+(\hbar\omega_p/E_g)^2$. It is clear that $\varepsilon(0)$ is inversely proportional to E_g. We can determine E_g from this expression by using the values of $\varepsilon_1(0)$ and the plasma energy $\hbar\omega_p$.

3.5. Nonlinear optical response

In a crystal, the polarization P can be expressed as a Taylor expansion of the macroscopic electric filed, E, according to

$$P_i = P_i^s + \sum_j \chi_{ij}^{(1)} E_j + \sum_{j,k} \chi_{ijk}^{(2)} E_j E_k + \cdots,$$

where indices i, j, k denote the Cartesian components, P^s is the zero-field (spontaneous) polarization vector, $\chi_{ij}^{(1)}$ is the linear dielectric susceptibility (second-rank tensor), and $\chi_{ijk}^{(2)}$ is the second-order nonlinear optical susceptibility (third-rank tensor). The higher order terms can also be calculated but in this section we are only interested in the second-order optical response. Since the $CdGeAs_2$ compound is belong to the point group $\overline{4}2m$, there are only two independent components of the SHG tensor, namely, 123 and 312 components (1, 2 and 3 refer to the x-, y- and z-axis, respectively, which are chosen along the cubic axes). In the static limit, the two components are equal according to Kleninman "permutation" symmetry, which dictates additional relations between tensorial components beyond the purely crystallographic symmetry.

In this section, we focus on the results for the different contributions to the imaginary part of $\chi_{312}^{(2)}(-2\omega;\omega,\omega)$ and the SHG susceptibility in the zero frequency limit. The nonlinear optical properties are more sensitive to small changes in the band structure than the linear optical properties. Hence, any anisotropy in the linear optical properties is enhanced in the nonlinear spectra. This is attributed to the fact that the second harmonic response involves 2ω resonance in addition to the usual 1ω resonance. In order to better understand the origin of the relative magnitudes of the intraband and interband contributions, we now consider the frequency-dependent $\chi^{(2)}(-2\omega;\omega,\omega)$ functions, or, more precisely, their imaginary part $\mathrm{Im}\,\chi^{(2)}(-2\omega;\omega,\omega)$, from which the real and in particular its static value can be obtained by a Kramers–Kronig relations [67]. Different contributions to the imaginary part of $\chi_{312}^{(2)}(-2\omega;\omega,\omega)$ are presented in Fig. 5. We reveal that all SHG susceptibility is vanished at zero energy. Major SHG peaks occur between 1.0 eV and 8.0 eV. The 2ω terms start contributing at energy $\sim 1/2E_g$ and the 1ω terms for the energy values above E_g. In the low energy region (≤ 3 eV), the SHG optical spectra are dominated by the 2ω contributions. Beyond 3 eV the major contributions come from the 1ω terms. Only one peak near 1.42 eV possesses inter (2ω) transitions. At energy higher than 8.0 eV, the imaginary part of $\chi_{312}^{(2)}(-2\omega;\omega,\omega)$ drops to zero very fast. Both the inter (1ω) and intra (1ω) contributions in the energy region below 9.5 eV change signs several times. However, the inter (2ω) and intra (2ω) contributions in the most interesting energy region below 8 eV (for the Kramers–Kronig integral which gives the zero frequency value) do not change the sign (the former is negative, the latter is positive). This means that both inter (2ω) and intra (2ω) contributions to the static SHG are large and have opposite signs.

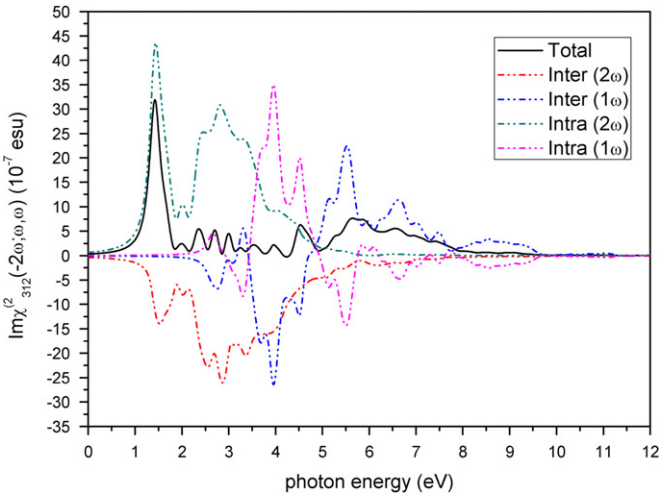

Fig. 5. Calculated total $\mathrm{Im}\,\chi_{312}^{(2)}(-2\omega;\omega,\omega)$ spectra along with the intra-(2ω)/(1ω) and inter-(2ω)/(1ω) band contributions.

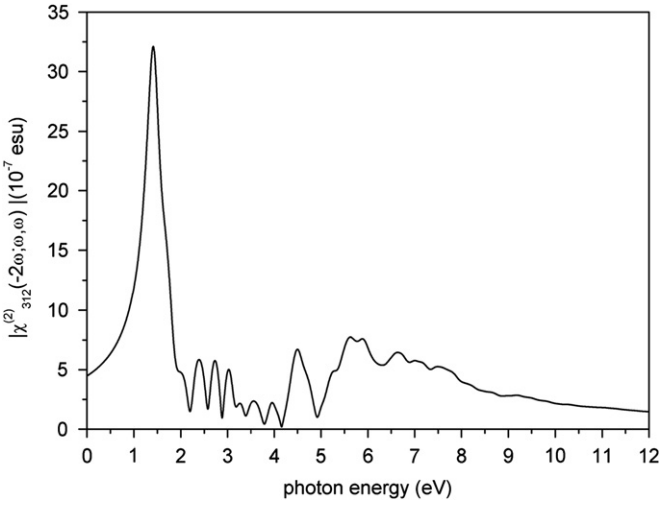

Fig. 6. Absolute value of the SHG susceptibility $|\chi_{312}^{(2)}(-2\omega;\omega,\omega)|$ for $CdGeAs_2$.

In Fig. 6 we plot the absolute value of the SHG susceptibility $|\chi_{312}^{(2)}(-2\omega;\omega,\omega)|$ for $CdGeAs_2$. The $\chi_{312}^{(2)}(-2\omega;\omega,\omega)$ component dominates in the spectrum for virtually all energies. The $|\chi_{312}^{(2)}(-2\omega;\omega,\omega)|$ is calculated from the $\mathrm{Im}\,\chi_{312}^{(2)}(-2\omega;\omega,\omega)$ and $\mathrm{Re}\,\chi_{312}^{(2)}(-2\omega;\omega,\omega)$. To our knowledge, the lack of experimental data prevents any conclusive comparison with experiment over a large energy range. We have succeeded in calculating the SHG susceptibility of $CdGeAs_2$ beyond zero frequency using a pseudopotential plane-wave method for the first time. Specially, the maximum value appears at 1.41 eV. Our calculated SHG susceptibility $\chi_{312}^{(2)}(0)=188$ pm/V at zero frequency, which is close to the experimental values of 186 ± 16 pm/V [74,75] and 236 pm/V [1]. Rashkeev et al. [37] have calculated the value of $\chi^2(0)$ in $CdGeAs_2$ (506 pm/V) which is higher than those experimental values and our calculated value above. The higher value of $\chi^2(0)$ is mainly due to the overcorrected scissors value. $CdGeAs_2$ has a smaller energy gap E_g than other chalcopyrite structure semiconductors;

we notice that the smaller band gap compound gives higher values of $\chi^{(2)}_{312}(0)$ [49,50]. However, the value of the SHG cannot be explained only by a small band gap. It is found that the intraband and interband contributions are also important to the second-order response.

4. Conclusion

In conclusion, we have presented results for the electronic, linear and nonlinear optical properties of $CdGeAs_2$ using a pseudopotential plane-wave method. Firstly, the structural parameters, including the internal coordinates, are relaxed, and excellent agreement is achieved with experimental results. Our results for the band structure and DOS show that $CdGeAs_2$ has a direct band gap with the calculated value to be 0.16 eV. The calculated total DOS and PDOS show that the valence band of $CdGeAs_2$ can be divided into three zones. To visualize the nature of the bond character, we calculate the total electronic charge density on the (110) plane of $CdGeAs_2$. We find that the charge density around the cation Cd is spherical in agreement with the previous papers and the bonds of Cd–As have more covalent part than those of Ge–As.

The DFT band structure fails to give reliable quantitative values for the band gaps of semiconductors. In our present work, we use the way in which we do not have to rely on experimental gap is to determine the self-energy using GW approximation. In this case the opening of the gap due to the GW correction can be used as scissor shift. The calculated energy gap is 0.35 eV at Γ point. This is substantially larger than the LDA value and closer to the experimental value. The corrected gap is used as scissor shift to calculate the linear and nonlinear optical properties.

Our results for the imaginary part of the frequency dependent dielectric function are labeled with letters and summarized. The origin of these peaks is due to the interband transitions of Cd-*sp* and Ge-*sp*. The most important quantity is the zero frequency limit $\varepsilon_1(0)$, which is found to be in good agreement with both experimental and theoretical data. We note that a smaller energy gap E_g yields a larger $\varepsilon_1(0)$ value. We have succeeded in calculating the SHG susceptibility of $CdGeAs_2$ beyond zero frequency using a pseudopotential plane-wave method for the first time. The intra- and inter-band contributions to the imaginary part of $\chi^{(2)}_{312}(-2\omega;\omega,\omega)$ are presented over a broad energy range. One could expect that the spectra structures in $\mathrm{Im}\,\chi^{(2)}_{312}(-2\omega;\omega,\omega)$ could be understood from the features of $\varepsilon_2(\omega)$. Unlike the linear optical spectra, the features in the SHG susceptibility are very difficult to identify from the band structure due to the presence of 2ω and 1ω terms. But we can use the linear optical spectra to identify the different resonance singularities leading to chief features in the SHG spectra. The first spectral band in $\mathrm{Im}\,\chi^{(2)}_{312}(-2\omega;\omega,\omega)$ between 0 and 3.5 eV is mainly originated from 2ω resonance and arises from the first structure in $\varepsilon_2(\omega)$. The second band between 3.5 and 5 eV is associated with interference between 1ω resonance and 2ω resonance and arises from the high structure in $\varepsilon_2(\omega)$. The last band from 5 to 9.5 eV is mainly due to 1ω resonance and is associated with the tail in $\varepsilon_2(\omega)$. Our calculated SHG susceptibility $\chi^{(2)}_{312}(0)=188$ pm/V at zero frequency, which is close to the experimental values. The smaller energy band gap compounds have larger values of $\chi^{(2)}_{312}(0)$ in agreement with the experimental measurements and other theoretical calculations.

Acknowledgments

This work was supported by the National Natural Science Foundation General and Key Programs of China (Grant no. 50732005) and the 863 High-Tech Program of China (Grant no. 2007AA032443).

References

[1] R.L. Byer, H. Kildal, R.S. Feigelson, Appl. Phys. Lett. 19 (1971) 237.
[2] A. Shileika, Surf. Sci. 37 (1973) 730.
[3] I.P. Akimchenko, A.S. Borshchevskii, V.S. Ivanov, Sov. Phys. Semicond. 7 (1973) 98.
[4] P.G. Schunemann, K.L. Schepler, P.A. Budni, Mater. Res. Soc. Bull. 23 (1998) 45.
[5] A. Zakel, J.L. Blackshire, P.G. Schunemann, S.D. Setzler, J. Goldstein, S. Guha, Appl. Opt. 41 (2002) 2299.
[6] K.L. Vodopyanov, P.G. Schunemann, Opt. Lett. 23 (1998) 1096.
[7] K.L. Vodopyanov, G.M.H. Knippels, A.F.G. van der Meer, J.P. Maffetone, I. Zwieback, Opt. Commun. 202 (2002) 205.
[8] P.G. Schunemann, T.M. Pollak, J. Cryst. Growth 174 (1997) 272.
[9] P.G. Schunemann, T.M. Pollak, Mater. Res. Soc. Bull. 23 (1998) 23.
[10] P.G. Schunemann, S.D. Setzler, T.M. Pollak, A.J. Ptak, T.H. Myers, J. Cryst. Growth 225 (2001) 440.
[11] K. Nagashio, et al., J. Cryst. Growth 269 (2004) 195.
[12] H. Pfister, Acta Crystallogr. 11 (1958) 221.
[13] L. Cervinka, J. Kaspar, Czech. J. Phys. B 20 (1970) 101.
[14] A.A. Vaipolin, Fiz. Tverd. Tela 15 (1973) 1430.
[15] S.C. Abrahams, J.L. Bernstein, J. Chem. Phys. 61 (1974) 1140.
[16] F.P. Baumgartner, M. Lux-Steiner, E. Bucher, J. Electron. Mater. 19 (1990) 777.
[17] S.F. Marenkin, V.M. Novotortsev, K.K. Palkina, S.G. Mikhailov, V.T. Kalinnikov, Inorg. Mater. 40 (2004) 93.
[18] V.M. Novotortsev, K.K. Palkina, S.G. Mikhailov, A.V. Molchanov, L.I. Ochertyanova, S.F. Marenkin, Inorg. Mater. 41 (2005) 439.
[19] A.S. Borshchevskii, N.E. Dagina, A.A. Lebedev, K. Ovegov, I.K. Polushina, Yu.V. Rud, Fiz. Tekh. Poluprovodn. 10 (1976) 1905.
[20] G. Krivaite, A.S. Borshchevskii, A. Sileika, Phys. Stat. Sol. (b) 57 (1973) K39.
[21] R. Madelon, M. Shaimi, A. Hairie, E. Paumier, B. Mercey, Solid State Commun. 50 (1984) 545.
[22] R. Madelon, E. Paumier, A. Hairie, Phys. Stat. Sol. (b) 165 (1991) 435.
[23] A. Abraham, V. Vorlicek, M. Zavetova, Czech. J. Phys. B 18 (1968) 958.
[24] N.A. Goryunova, E.F. Gross, L.B. Zlatkin, E.K. Ivanov, J. Non-Cryst. Solids 4 (1970) 57.
[25] L.B. Zlatkin, Yu.F. Markov, A.I. Stekhanov, M.S. Shur, J. Phys. Chem. Solids 31 (1970) 567.
[26] G.D. Holah, A. Miller, W.D. Dunnett, G.W. Iseler, Solid State Commun. 23 (1977) 75.
[27] G.W. Iseler, H. Kildal, N. Menyuk, J. Electron. Mater. 7 (1978) 737.
[28] K.S. Hong, R.F. Speyer, R.A. Condrate Sr., J. Phys. Chem. Solids 51 (1990) 969.
[29] D.W. Fischer, M.C. Ohmer, J.E. Mccrae, J. Appl. Phys. 81 (1997) 3579.
[30] I. Zwieback, D. Perlov, J.P. Maffetone, W. Ruderman, Appl. Phys. Lett. 73 (1998) 2185.
[31] L.H. Bai, N.Y. Garces, N.Y. Yang, P.G. Schunemann, S.D. Setzler, T.M. Pollak, L.E. Halliburton, N.C. Giles, Mater. Res. Soc. Symp. Proc. 744 (2003) 537.
[32] L.H. Bai, J.A. Poston Jr., P.G. Schunemann, K. Nagashio, R.S. Feigelson, N.C. Giles, J. Phys.: Condens. Matter 16 (2004) 1279.
[33] L.H. Bai, N.C. Giles, P.G. Schunemann, J. Appl. Phys. 97 (2005) 023105.
[34] L.H. Bai, C.C. Xu, N.C. Giles, K. Nagashio, R.S. Feigelson, J. Appl. Phys. 99 (2006) 013512.
[35] K.T. Zawilski, P.G. Schunemann, T.M. Pollak, J. Cryst. Growth 310 (2008) 1897.
[36] H. Kildal, G.W. Iseler, Phys. Rev. B 19 (1979) 5218.
[37] S.N. Rashkeev, S. Limpijumnong, W.R.L. Lambrecht, Phys. Rev. B 59 (1999) 2737.
[38] Yu.M. Andreev, V.G. Voevodin, P.P. Geiko, A.I. Gribenyukov, A.P. Dyadkin, S.V. Pigulskii, A.I. Starodubtsev, Sov. J. Quantum Electron. 17 (1987) 491.
[39] H. Kildal, Phys. Rev. B 10 (1974) 5082.
[40] S.I. Borisenko, G.F. Karavaev, Sov. Phys. J. 25 (1982) 65.
[41] J.E. Jaffe, A. Zunger, Phys. Rev. B 29 (1984) 1882.
[42] P. Zapol, R. Pandey, M. Seel, J.M. Recio, M.C. Ohmer, J. Phys.: Condens. Matter 11 (1999) 4517.
[43] S. Limpijumnong, W.R.L. Lambrecht, Phys. Rev. B 65 (2002) 165204.
[44] T.R. Paudel, W.R.L. Lambrecht, Phys. Rev. B 78 (2008) 085214.
[45] L.W. Qiang, Y.C. Hui, S. Liang, Z.C. Qiang, M.T. Hui, S. Yu, Chin. J. Struct. Chem. 28 (2009) 553.
[46] Y. Yu, B.J. Zhao, S.F. Zhu, T. Gao, H.J. Hou, Solid State Sci. 13 (2011) 422.
[47] L. Bai, Z.S. Lin, Z.Z. Wang, C.T. Chen, M.H. Lee, J. Chem. Phys. 120 (2004) 8772.
[48] A. Chahed, O. Benhelal, S. Laksari, B. Abbar, B. Bouhafs, N. Amrane, Physica B 367 (2005) 142.
[49] A.H. Reshak, Physica B 369 (2005) 243.
[50] A.H. Reshak, S. Auluck, PMC Phys. B 1 (12) 10.1186/1754-042.
[51] L. Bai, Z.S. Lin, Z.Z. Wang, C.T. Chen, J. Appl. Phys. 103 (2008) 083111.
[52] T. Ouahrani, A.H. Reshak, A. Otero de la Roza, M. Mebrouki, V. Luana, R. Khenata, B. Amrani, Eur. Phys. J. B 72 (2009) 361.
[53] L. Hedin, S. Lundquvist, in: H. Ehrenreich, F. Seitz, D. Turnbull (Eds.), Solid State Physics: Advances in Research and Applications, vol. 23, Academic, New York, 1969, p. 1.
[54] X. Gonze, J.-M. Beuken, R. Caracas, F. Detraux, M. Fuchs, G.-M. Rignanese, L. Sindic, M. Verstraete, G. Zerah, F. Jollet, M. Torrent, A. Roy, M. Mikami, Ph. Ghosez, J.-Y. Raty, D.C. Allan, Comput. Mater. Sci. 25 (2002) 478 〈http://www.abinit.org〉.
[55] S. Goedecker, SIAM J. Sci. Comput. (USA) 18 (1997) 1605.
[56] M.C. Payne, M.P. Teter, D.C. Allan, T.A. Arias, J.D. Joannopoulos, Rev. Mod. Phys. 64 (1992) 1045.
[57] X. Gonze, Phys. Rev. B 54 (1996) 4383.

[58] M. Fuchs, M. Scheffler, Comput. Phys. Commun. 119 (1999) 67.
[59] J.P. Perdew, Y. Wang, Phys. Rev. B 45 (1992) 13244.
[60] D.M. Ceperley, B.J. Alder, Phys. Rev. Lett. 45 (1980) 566.
[61] R.W. Godby, M. Schluter, L.J. Sham, Phys. Rev. B 37 (1988) 10159.
[62] C.S. Wang, B.M. Klein, Phys. Rev. B 24 (1981) 3417.
[63] J.E. Sipe, A.I. Shkrebtii, Phys. Rev. B 61 (2000) 5337.
[64] J.L. Shay, J.H. Wernick, Ternary Chalcopyrite Semiconductors: Growth, Electromic Properties and Applications, Pergamon, Oxford, 1974.
[65] J. Lin, M.H. Lee, Z.P. Liu, C.T. Chen, C.J. Pickard, Phys. Rev. B 60 (1999) 13380.
[66] M. Oshikiri, F. Aryasetiawan, Phys. Rev. B 60 (1999) 10754.
[67] H. Tributsch, Z. Naturforsch. A 32A (1977) 972.
[68] R. Pandey, M.C. Ohmer, J.D. Gale, J. Phys.: Condens. Matter 10 (1998) 5525.
[69] A. MacKinnon, Physics of Ternary Compounds, Landolt–Börnstein, New Series, Group III, vol. 17 (Part h), Springer, Berlin, 1985, pp. 97–99.
[70] A.H. Reshak, Eur. Phys. J. B 47 (2005) 503.
[71] A.H. Reshak, S. Auluck, Physica B 388 (2007) 34.
[72] A. Shaukat, Y. Saeed, N. Ikram, H. Akbarzadeh, Eur. Phys. J. B 62 (2008) 439.
[73] D.R. Penn, Phys. Rev. 128 (1962) 2093.
[74] E. Tanaka, K. Kato, Mater. Res. Soc. Symp. Proc. 484 (1998) 475.
[75] G.D. Boyd, E. Buehler, F.G. Storz, J.H. Wernick, IEEE J. Quantum Electron. QE-8 (1972) 419.